A Model of the Pumping Action Between the Teeth of High-Speed Spur and Helical Gears

C. Milian, J.P. Distretti, P. Leoni, and P. Velex

Summary

With the evolution of the high-speed gearbox market for high-power turbo units, mesh velocity is increasing year after year.

For a high-speed gearbox, an important part of power losses is due to the mesh. A global estimation is not possible and an analytical approach is necessary with evaluations of three different origins of power losses: friction in mesh contact, gear windage and pumping effect between teeth.

This article thoroughly explains the last subject. The theoretical model, which is developed, is a useful tool for analyzing the physical effect of pumping in mesh. It can be used to optimize the choice of the gear parameters that influence heat generation and predict temperature distribution along the teeth for the design of thermal lead corrections.

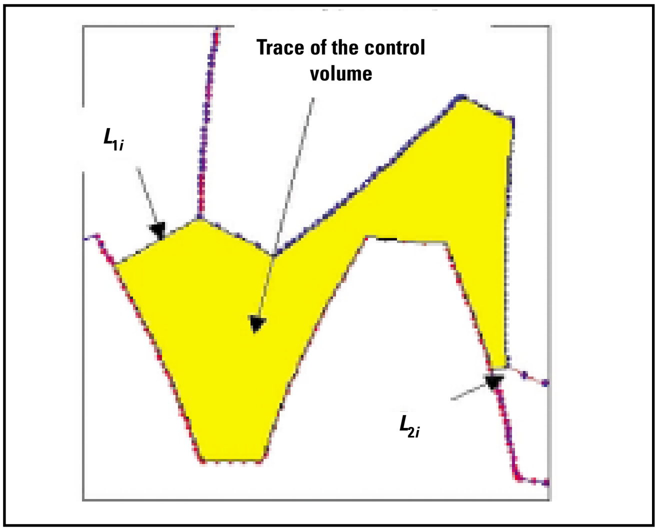

Figure 1—Definition of the control volume and exit flow areas.

Abstract

An approximate one-dimensional hydrodynamic analysis of the air-lubricant pumping between gear teeth is presented. Assuming an isentropic compression and considering the air-lubricant mixture as a perfect gas, the continuity equation is applied to the control volume limited by the surfaces of the teeth. Once critical conditions are reached, the exit flows are bounded and the gas in the control volume is compressed and heated. The temperature variations along the tooth face delivered by the model compare favorably with those measured on two industrial turbo-gear sets. It is therefore concluded that the proposed approach can provide useful indications at the design stage on the air-lubricant compression between the teeth and on related heating problems.

Introduction

The gear temperature and temperature distribution are important parameters for the evaluation of scoring and scuffing risks as well as tooth load distributions across face widths. However, the mechanism of heat generation and cooling by the lubricant in wide-faced, high-speed geared transmissions remains one of the lesser understood phenomena related to gear design. During the time period in which a tooth first crosses the addendum cylinder and proceeds to fill up most of the volume between the teeth, a fraction of the air and the lubricant in the tooth space is expelled from the gear.

The time duration of a mesh period in turbo-machinery is extremely short, and the air-lubricant mixture can be significantly compressed and heated. Rosen (Ref. 1) computed the velocity of the air flow in spur gears using an incompressible flow theory and found that the air velocity approaches sonic conditions for a particular gear set, and this corresponded to an experimentally observed rise in noise. Smith (Ref. 2) notes that noise can be generated when oil is trapped in the roots of wide-faced gears, and the acoustic measurements of Houjoh and Umezawa (Ref. 1) led to the conclusion that the pulsating flow from the gear pumping action can be a significant noise source.

The thermal issues associated with fluid being expelled between the teeth are discussed in the classic handbooks of Buckingham (Ref. 4) and Dudley (Ref. 5). Pechersky and Wittbrodt (Ref. 6) have presented incompressible and compressible fluid flow analyses between meshing spur gear teeth, and they found substantial pressure and temperature rises. Butsch (Ref. 7) developed a compressible flow model for spur gears and showed that sonic conditions can lead to compression and heat generation in the air-lubricant mist. In a series of papers, Matsumoto et al. (Ref. 8–9) have analyzed thermal behavior of high-speed helical gears and obtained uneven temperature distributions along tooth faces in accordance with their experimental findings.

The objective of this article is to present a simplified hydrodynamic analysis of the pumping action resulting from the meshing of wide-faced helical gears. Compressible flows are considered, and the fluid velocity, pressure and temperature along the face width are estimated. The calculations require a detailed analysis of involute and helical geometries in order to determine the proper mesh region volumes and exit flow areas. The agreement between the measured temperatures on two different gear sets and the predicted figures is reasonable and proves the interest of the proposed method at the design stage.

Hydrodynamic Model

The equations for the fluid velocity, pressure and temperature are derived by applying the continuity equation for a perfect gas to a time-varying control volume. Considering an isentropic transformation, one gets:

$$\frac{dp}{p} = \gamma \frac{d\rho}{\rho} \tag{1}$$

where p is the pressure, ρ the fluid density and γ the isentropic coefficient ($\cong 1.4$).

The control volume V, i.e., the inter-tooth volume, varies during rotation. It is bounded by the flanks of two adjacent pinion teeth, their bottomland and the surface of the meshing gear tooth (Figure 1). One-dimensional flow is assumed (Ref. 6) and the integral form of the continuity equation applied to the control volume V reads:

$$\frac{\partial}{\partial t}\int_{(V)} \rho dV + \int_{(S)} \rho v.ndS = 0 \tag{2}$$

with v as fluid velocity with respect to the exit surface S and n as unit vector to S.

Assimilating a helical gear to a series of staggered spur gears, the hydrodynamic model for the pumping effect between the teeth is made of a succession of discrete fluid pockets, each with constant state variables (Figure 2). If one elemental spur gear (or one pocket) is isolated, the air-lubricant mixture is ejected through the time-varying inter-tooth clearances L_{1i}, L_{2i} and across the axial discharge front and rear surfaces perpendicular to the apparent plane. Three different cases have to be distinguished: i) the first pocket in the direction of the meshing progress (pocket 1) which is connected to the ambient at one side and to pocket 2 at the other side, ii) any generic pocket i linked to pockets i–1 and i+1, and iii) the extreme one (pocket N) in connection with pocket N–1 and the ambient.

For any pocket i, Equation (2) is discretized as:

$$\rho_i \frac{dV_i}{dt} + V_i \frac{d\rho_i}{dt} + \alpha\rho_{i-1} S_{Ai-1} U_{Ai-1} + \delta\rho_{i+1} S_{Ai+1} U_{Ai+1} + (S_{Ri1} + S_{Ri2})U_{Ri} = 0 \tag{3}$$

which, after multiplying by $\frac{1}{\rho_i V_i}$ and introducing (1) is finally rewritten as:

$$\frac{1}{V_i}\frac{dV_i}{dt} + \frac{1}{\gamma P_i}\frac{dP_i}{dt} + \frac{1}{V_i}\left(\frac{P_e}{P_i}\right)[\alpha\rho_{i-1} S_{Ai-1} U_{Ai-1} + \delta\rho_{i+1} S_{Ai+1} U_{Ai+1} + (S_{Ri1} + S_{Ri2})U_{Ri}] = 0 \tag{4}$$

with:

P_i :	pressure in pocket i
P_e :	ambient pressure
S_{Ai-1}, S_{Ai+1} :	axial discharge areas
S_{Ri} :	radial discharge area
U_{Ai-1} , U_{Ai+1} :	axial speeds
U_{Ri} :	radial speed
V_i :	instantaneous volume of pocket i

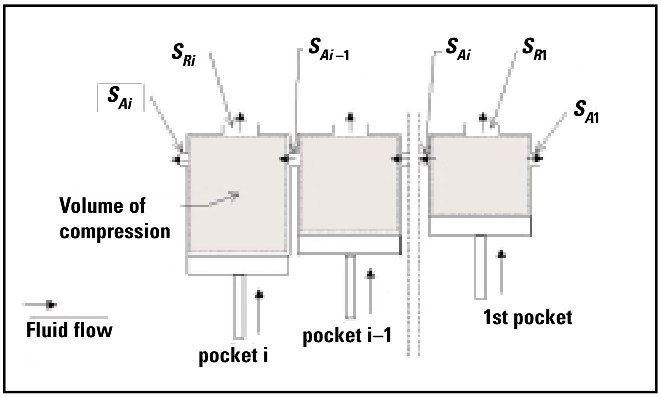

Figure 2—Discrete hydrodynamic model for helical gears.

Table 1—Gear data (Example for the calculation of radial clearance and axial exit area).		
Tooth number	47	103
Module (mm)	6.8	
Pressure angle (°)	22.5	
Helix angle (°)	0	
Profile shift coefficient	0.291	0.322
Addendum coefficient	1	1
Dedendum coefficient	1.475	1.474

P. Leoni *is the managing director of the high-speed gearbox division of Flender Group in Illkirch-Graffenstaden, France.*

Phillipe Distretti *is an engineer and the R&D manager of Flender-Graffenstaden.*

Phillipe Velex *is a professor at the engineering school INSA, in Lyon, France. He's working in LaMCoS, a research laboratory in Lyon, and specializing in tribology and gears.*

Cedric Milian*, a mechanical engineer, is working in R&D at Flender-Graffenstaden.*

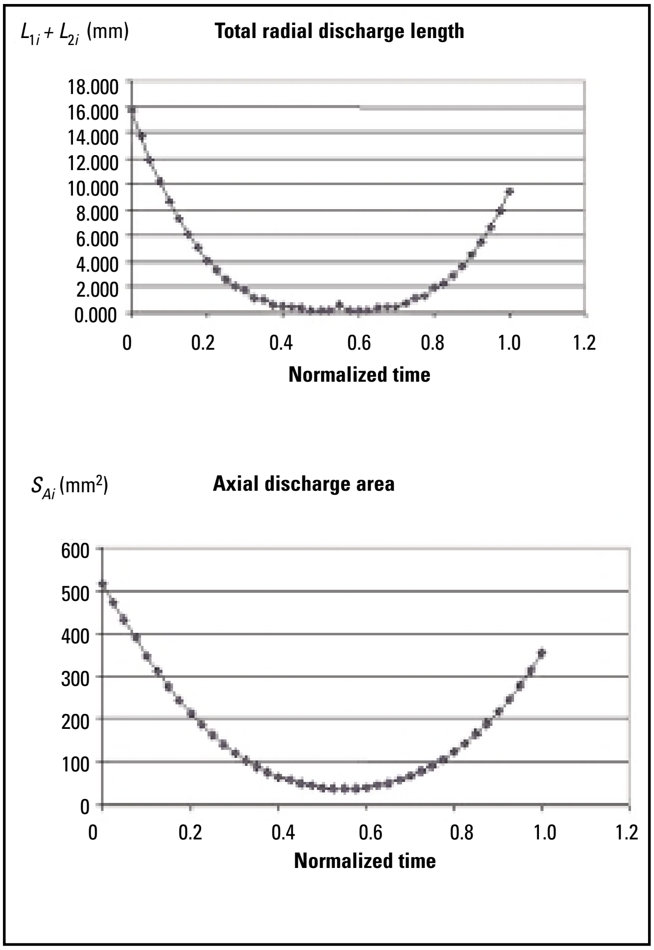

Figure 3—Evolution of radial clearances and axial exit area.

Figure 4—High speed test rig.

Table 2—Gear Data (Case 1).		
Tooth number	47	117
Module (mm)	7	
Pressure angle (°)	20	
Helix angle (°)	12.75	
Profile shift coefficient	0.16	0.05
Addendum coefficient	0.9919	0.9925
Dedendum coefficient	1.47921	1.47885

$$\alpha = 0 \text{ if } i = 1,\ \alpha = -\left(\frac{P_e}{P_i}\right)^{\frac{-1}{\gamma}} \text{ if } i \neq 1$$

$$\delta = 1 + \left(\frac{P_e}{P_i}\right)^{\frac{-1}{\gamma}} \text{ if } i = 1,\ \delta = \left(\frac{P_e}{P_i}\right)^{\frac{-1}{\gamma}} \text{ if } i \neq 1 \text{ and } N,$$

$$\delta = 1 \text{ if } i = N$$

Connections between the different volumes are ensured by writing the conservation of mass flow at all interfaces between any pair of pockets. Equation (4) is a non-linear differential equation of major unknown P_i, pressure in pocket i. $\frac{1}{V_i}\frac{dV_i}{dt}$ as well as the exit surfaces S_{Ai-1}, S_{Ai+1}, S_{Ri} depend on the relative position of the meshing gears and pinion teeth and have to be evaluated step-by-step in time. The involute profiles of the teeth of the pinion and the gear at one arbitrary initial position are discretized. The axial discharge area S_{Ai} is obtained by numerical integration, and clearances L_{1i}, L_{2i} are set to be the minimum distance between the tip corners of gear teeth and the pinion profiles (Figure 1). The volume V_i and the flow areas associated with an elemental spur gear (or pocket) of width b are deduced by:

$$V_i = S_{Ai} b \tag{5-1}$$

$$S_{Ri1} = L_{1i} b \quad S_{Ri2} = L_{2i} b \tag{5-2}$$

The profile coordinates are recalculated after rotating the pinion of an angle $\Delta\theta_p = \Omega_1 \Delta t$ and the gear of the corresponding angle $\Delta\theta_g = \Omega_2 \Delta t$. The volume, the exit areas and the volume time-variation for all pockets are then determined by using (5-1), (5-2) and $\frac{dV_i}{dt}$ and $\frac{V_i(t+\Delta t) - V_i(t)}{\Delta t}$. For one elemental spur gear, Figure 3 represents the evolution of the total inter-tooth clearance $L_{1i} + L_{2i}$ along with the volume V_i over one complete pumping stroke (the gear data are in Table 1).

Temperature, fluid density and mass flows are derived from the following equations for perfect gases:

$$T(t) = T(t - \Delta t)\left[\frac{P(t-\Delta t)}{P(t)}\right]^{\frac{1-\gamma}{\gamma}} \tag{6-1}$$

$$\rho(t) = \rho(t - \Delta t)\left[\frac{P(t-\Delta t)}{P(t)}\right]^{\frac{1}{\gamma}} \tag{6-2}$$

$$Q(t) = \rho(t)U(t)S(t) \tag{6-3}$$

The mass flow $Q(t)$ through any surface $S(t)$ has to be compared with the maximum value, which can be expelled, i.e., the mass flow for sonic (critical) conditions (Ref. 7).

$$Q_{\max}(t) = \frac{1}{r}\left(\frac{2}{\gamma+1}\right)^{\frac{1}{\gamma-1}} \sqrt{\frac{2\gamma r}{\gamma+1}}\ \frac{P(t)}{\sqrt{T(t)}}\ S(t) \tag{7}$$

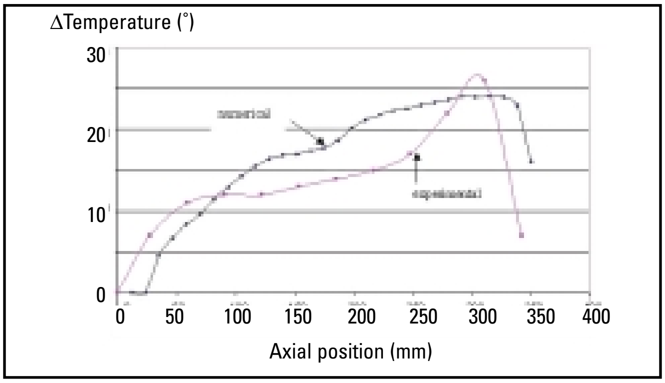

Figure 5—Temperature variations versus axial position—Case 1.

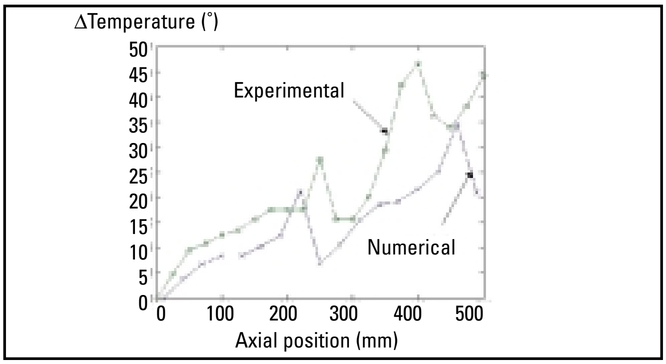

Figure 6—Temperature variations versus axial position—Case 2.

with $r = R/M$ as fluid constant, R as molar constant (8.3144 J.mole^{-1} K^{-1}) and M as molar mass.

If the calculated output flow exceeds the critical value Q_{max} (t), the fluid between the teeth is compressed and its state variables are re-evaluated iteratively by using a Newton-Raphson technique until the continuity equation and the critical mass flow condition are simultaneously satisfied.

Experiments on High-Speed Gear Sets

The test-rig is an open-loop, single-stage reduction system (Figure 4). The gears are lubricated by jets, and shafts are mounted on hydrodynamic bearings. Power is supplied by a 1500 kW electric motor, which operates the test stand through a speed multiplier from 0 rpm to a maximum speed of 26,000 rpm on the input shaft. In what follows, all tests were conducted in no-load conditions. Two gear sets were tested (data is given in Tables 2 and 3) at high-speed, respectively 9,267 rpm (Case 1) and 8,962 rpm (Case 2) on the pinion shaft.

It can be shown that, for high-speeds, the temperature distribution in the gear teeth does not depend on the angular coordinate. Since longitudinal tooth modifications are the major concern of the present work, only axial temperature distributions have been measured. Temperatures were sensed by several thermocouples along the face width as shown in Figure 4. The thermocouple heads were located at a distance of approximately 1 mm from the tooth topland. In such conditions, the absolute temperatures within the air-lubricant mixture or at the tooth surface cannot be obtained, but it is believed that realistic relative variations can be derived. Figures 5 and 6 show the experimental temperatures versus axial positions and the corresponding numerical results. The pumping of the fluid between the teeth leads to over-

Table 3—Gear Data (Case 2).

Tooth number	52	79
Module (mm)	6.8	
Pressure angle (°)	22.5	
Helix angle (°)	10	
Profile shift coefficient	0.198	0.21
Addendum coefficient	0.9891	0.9894
Dedendum coefficient	1.47469	1.47507

heating of the gear side close to the trailing edge, which, in Case 2, probably distorts mating teeth and imposes longitudinal shape modifications. It is also shown that a groove at mid-face width interrupts the compression process and reduces heat generation along the face width. For the two examples, a reasonable agreement is observed on the relative temperature distributions, and it is proven that the proposed simplified approach brings useful qualitative indications in terms of the system sensitivity to the compression-heating mechanism.

Conclusion

A one-dimensional approximation of the air-lubricant flow caused by the meshing of high-speed, wide-faced helical gears is presented. The results show that fluid velocity can reach high rates and, in certain cases, sonic conditions can be obtained. The air-lubricant flow is therefore compressed and heated along the axial direction. The theoretical predictions have been compared with the experimental evidence from two turbo-gear sets. It is found that the simulated relative temperature variations across tooth faces agree reasonably well with the measured data. In the context of tooth lead modifications, the proposed model can bring useful indications on modification design and on the influence of changing geometrical gear parameters. However, the model discussed in this paper is based on several important approximations, the most important being the assumption of one-dimensional flow through discrete elements. Further research is under way in order to relax these approximations and consider continuous flows between moving boundaries.

References

1. Rosen, M.W., "The Noises of Two Spur Gear Tansmissions," NOTS TP 2293, NAVORD Report 6569, 1959.
2. Smith, J.D., "Gear noise and vibration," Marcel Dekker Inc., 186 p., 1999.
3. Houjoh, H. and K. Umezawa. "The Sound Radiated from Gears (On the Existence of Aerodynamic Sound)," *JSME Int. Journal*, Vol. 30, No. 259, pp. 153–160, 1987.
4. Buckingham, E. "Manual of Gear Design," *Machinery*, New York, 1935.
5. Dudley, D.W. *Handbook of Practical Gear Design*, McGraw-Hill, New York, NY, 1984.
6. Pechersky, M.J., and M.J. Wittbrodt. "An Analysis of Fluid Flow Between Meshing Spur Gear Teeth," *Proc. 5th ASME Power Trans. Gearing Conf.*, Chicago, pp. 335–342, 1989.
7. Butsch, M. "Hydraulische Verluste Schnell-Laufender Stirnradgetriebe," (Bericht 240), University IMK of Stuttgart, 1989.
8. Matsumoto, S., B. Asanabe, K. Takano and M. Yamamoto, "Evaluation Method of Power Loss in High-Speed Gears," *Proc. JSLE Int. Trib. Conf.*, pp. 1,165–1,170, 1985.
9. Matsumoto, S., Y. Tozaki and K. Sudoh, "Temperature Distribution in Tooth and Blanks of Ultra High Speed Gears," *Proc. JSME Int. Conf. Motion Power Trans.*, Hiroshima, pp. 496–501, 1991.